ELSEVIER

Materials Chemistry and Physics 62 (2000) 164–168

MATERIALS CHEMISTRY AND PHYSICS

www.elsevier.com/locate/matchemphys

Effects of additives and secondary phases on the sintering behavior of zinc oxide-based varistors

Chung-Hsin Lu*, Ning Chyi, Hsi-Wu Wong, Wen-Jeng Hwang

Department of Chemical Engineering, National Taiwan University, Taipei, Taiwan

Received 27 October 1998; received in revised form 2 July 1999; accepted 6 July 1999

Abstract

The influence of additives and secondary phases on the sintering behavior of zinc oxide-based varistors has been investigated in this study. Addition of Bi_2O_3 and Sb_2O_3 to ZnO results in rapid shrinkage of the specimens at around 1000°C. This rapid shrinkage is attributed to the reaction between the pyrochlore phase and ZnO. This reaction has been verified by investigating the system of ZnO and a synthesized pyrochlore phase $ZnBi_{1.5}Sb_{1.5}O_7$. This pyrochlore phase has a cubic symmetry, with a lattice parameter $a_o = 10.4438$ Å. $ZnBi_{1.5}Sb_{1.5}O_7$ is found to react with ZnO at 1000°C to lead to the formation of Bi_2O_3, which accelerates the sintering rate of ZnO through a liquid-phase sintering mechanism. On the other hand, the spinel phase α-$Zn_7Sb_2O_{12}$ hinders the sintering process as well as the grain growth of ZnO.

Keywords: Zinc oxide; Pyrochlore phase; Sintering; Microstructure

1. Introduction

Zinc oxide has been widely used to fabricate varistors since 1970s because of its excellent non-ohmic property [1]. Varistors are important protection devices against voltage surges in solid-state devices and electrical power generation systems [2]. To improve the electrical characteristics of varistors, considerable research efforts have been devoted to study the effects of adding small amounts of various additives to ZnO [3–7]. The most commonly used additives are Bi_2O_3, Sb_2O_3, Co_3O_4, MnO_2, Cr_2O_3, and NiO. Each of these additives plays a different role in enhancing the non-ohmic property of ZnO [8]. However, the presence of these additives results also in the formation of secondary phases in ZnO [9–11] and different microstructures [12,13]. The types of secondary phases formed depend on the added amount and the type of additive. In general, pyrochlore phase $ZnBi_{1.5}Sb_{1.5}O_7$ and spinel phase α-$Zn_7Sb_2O_{12}$ are found to be the two major compounds coexisting with ZnO [10].

Although the effects of additives on the electrical properties and microstructure of ZnO have been explored, how these additives and secondary phases influence the sintering of ZnO, remains unclear. For obtaining highly densified ZnO-based varistors, the basic study of the sintering phenomena is crucial. Hence, the purpose of the present study is to investigate the sintering behavior of ZnO-based varistors. The additives used in this study are Bi_2O_3, Sb_2O_3, and their resultant compounds with ZnO (pyrochlore phase $ZnBi_{1.5}Sb_{1.5}O_7$ and spinel phase α-$Zn_7Sb_2O_{12}$). Since the preparation of $ZnBi_{1.5}Sb_{1.5}O_7$ has not yet been investigated in detail, the formation process of $ZnBi_{1.5}Sb_{1.5}O_7$ was studied first. Then, the synthesized pyrochlore phase was added to ZnO. The phase evolution and microstructural development of ZnO, with additives added during sintering, were examined.

2. Experimental

Pyrochlore phase $ZnBi_{1.5}Sb_{1.5}O_7$ and spinel phase α-$Zn_7Sb_2O_{12}$ were prepared by using reagent grade ZnO, Bi_2O_3, and Sb_2O_3 as raw materials. These raw materials were weighed according to the desired composition, and ball-milled, using zirconium oxide balls, in ethanol for 48 h. The mixed slurry was dried at about 60°C in an evaporator. The dried powders were then pressed and calcined. After 1000°C calcination for 4 h, pure $ZnBi_{1.5}Sb_{1.5}O_7$ was obtained, while pure α-$Zn_7Sb_2O_{12}$ was produced after 900°C calcination for 4 h. The ZnO powder was then mixed and ball-milled with the additives of Bi_2O_3, Sb_2O_3, $ZnBi_{1.5}Sb_{1.5}O_7$, and α-$Zn_7Sb_2O_{12}$. The mixing ratio for each specimen is listed in Table 1. In the ZY3 and ZY4

---

*Corresponding author. Tel.: +886-2-3635230; fax: +886-2-3623040

0254-0584/00/$ – see front matter © 2000 Elsevier Science S.A. All rights reserved.
PII: S0254-0584(99)00166-2

Table 1
Composition of the mixtures of ZnO comprising various additives

Sample	ZnO	Bi_2O_3	Sb_2O_3	Pyrochlore $ZnBi_{1.5}Sb_{1.5}O_7$	α-Spinel $Zn_7Sb_2O_{12}$
ZY1	99.5[a]	0.5	–	–	–
ZY2	98.5	0.5	1.0	–	–
ZY3	99.0	–	–	1.0	–
ZY4	99.0	–	–	–	1.0

[a] Molar ratio.

systems, 1 mol% $ZnBi_{1.5}Sb_{1.5}O_7$ and α-$Zn_7Sb_2O_{12}$ were added to ZnO, respectively. The dried powders were pressed into discs and heated at a rate of 10°C/min up to 1250°C.

The compounds formed in the quenched specimens were investigated by X-ray powder diffraction analysis (XRD). In order to calculate the relative fractions of different phases in the resultant compounds, intensities of the distinct diffraction peaks, associated with phases (101) for ZnO, (440) for $ZnBi_{1.5}Sb_{1.5}O_7$, (511) for α-$Zn_7Sb_2O_{12}$, (151) for β-$Zn_7Sb_2O_{12}$, and (201) for β-Bi_2O_3, were measured. The relative fraction of each compound was calculated from the ratio of the intensity of the specific diffraction peak of each compound to the sum of the intensity of the specific diffraction peak of all compounds. The sintering behavior of the samples was examined by a dilatometer. The microstructural evolution and particle size of the heated specimens were investigated by scanning electron microscopy (SEM), coupled with energy dispersive X-ray spectroscopy (EDS).

3. Results and discussion

3.1. Preparation of $ZnBi_{1.5}Sb_{1.5}O_7$

In order to determine the optimum condition for preparing $ZnBi_{1.5}Sb_{1.5}O_7$, the starting materials for $ZnBi_{1.5}Sb_{1.5}O_7$ were quenched at various temperatures and analyzed by XRD. The XRD patterns of quenched specimens are illustrated in Fig. 1. It is found that, at 500°C, only the constituent compounds are present. At 600°C, a small amount of Bi_3SbO_7 begins to form. At 800°C, $BiSbO_4$ and the pyrochlore phase $ZnBi_{1.5}Sb_{1.5}O_7$ begin to appear. The amount of $ZnBi_{1.5}Sb_{1.5}O_7$ increases rapidly with a rise in temperature, accompanied by a decrease in the contents of intermediate compounds. After heating at 1000°C, the formation of $ZnBi_{1.5}Sb_{1.5}O_7$ is almost complete.

For enhancing the purity of the obtained $ZnBi_{1.5}Sb_{1.5}O_7$, the starting materials were heated at 1000°C for 4 h. The XRD pattern of the obtained specimen is shown in Fig. 2. The hkl indexes, d-spacings, and relative intensities are listed in Table 2. All lines of the diffraction pattern of $ZnBi_{1.5}Sb_{1.5}O_7$ is indexed in terms of a cubic symmetry, with a lattice parameter $a_o = 10.4438$ Å. The observed d-values (d_{exp}) are also compared with the calculated d-values (d_{calc}), as listed in Table 2.

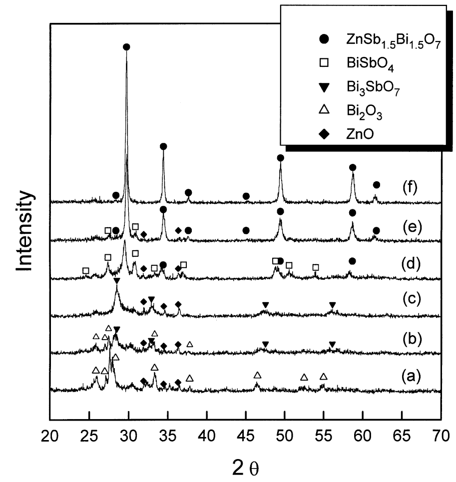

Fig. 1. X-ray diffraction patterns of the starting materials of $ZnBi_{1.5}Sb_{1.5}O_7$ quenched at various temperatures: (a) 500°C, (b) 600°C, (c) 700°C, (d) 800°C, (e) 900°C, and (f) 1000°C.

3.2. Influence of the presence of the secondary phases on sintering of ZnO

The sintering behavior of mixed specimens and pure ZnO is illustrated in Fig. 3. As shown in the figure, pure ZnO starts shrinking from about 700°C, and attains a final

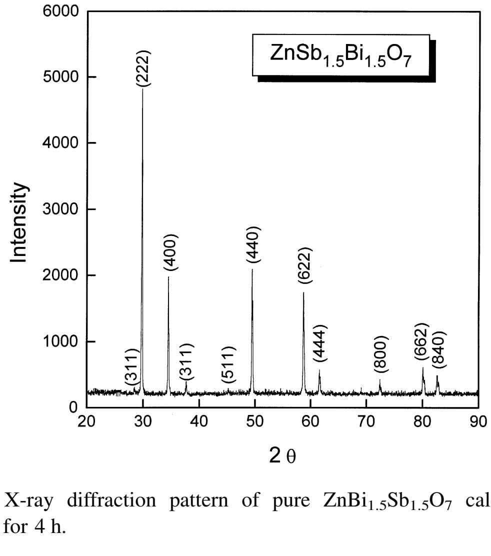

Fig. 2. X-ray diffraction pattern of pure $ZnBi_{1.5}Sb_{1.5}O_7$ calcined at 1000°C for 4 h.

Table 2
X-ray diffraction data of $ZnBi_{1.5}Sb_{1.5}O_7$

hkl	d_{exp} [a]	d_{calc} [b]	I/I_o
311	3.1499	3.1489	2
222	3.0125	3.0149	100
400	2.6093	2.6110	38
331	2.3964	2.3960	5
511	2.0078	2.0099	2
440	1.8448	1.8462	47
622	1.5739	1.5745	39
444	1.5068	1.5074	9
800	1.3057	1.3055	4
662	1.1973	1.1980	9
840	1.1672	1.1677	8

[a] Observed d-value obtained by experiment.
[b] Calculated d-value based on $a_o = 10.4438$ Å.

shrinkage of 14% at 1250°C. In the ZY1 system, which contains 0.5 mol% Bi_2O_3, the onset temperature for shrinkage is found to be reduced to 650°C and the final shrinkage at 1250°C reaches 18.5%. The decrease in the onset temperature for shrinkage and the increase in the shrinkage ratio are attributed to the presence of melting Bi_2O_3. As for the ZY2 and ZY3 systems, their shrinkage behaviors are very similar, exhibiting nearly overlapping shrinkage curves. In comparison with ZnO, these two systems exhibit a postponed shrinkage behavior. The onset temperature for shrinkage is found to be around 1000°C. However, at elevated temperatures, both systems exhibit a larger shrinkage ratio than ZnO. On the other hand, in the ZY4 system, which contains 1 mol% α-$Zn_7Sb_2O_{12}$ phase, the onset temperature for shrinkage increases further to 1050°C.

In order to examine the microstructural evolution in ZY2, ZY3, and ZY4 systems, the specimens were quenched at 1000°C and 1100°C during the heating process. At 1000°C, the microstructures of all four systems were found to be nearly identical, appearing highly porous, with a particle size of around 0.2 μm. This microstructural observation indicates that these specimens are not densified. A representative SEM photo (ZY2 system) is presented in Fig. 4(a). When the temperature is raised to 1100°C, the ZY2 and ZY3 systems rapidly become densified, but not ZY4. The typical microstructures of ZY2, ZY3, and ZY4, at 1100°C, are shown in Fig. 4(b,c, and d), respectively. Densified features can be observed clearly for the former two specimens, while ZY4 still exhibits a porous microstructure. In the ZY2 system, ZnO grains rapidly grow to a size of 6–8 μm, and some plate-like grains are also formed. The composition of these plate-like grains was identified by EDS and was found to be close to that of $Zn_7Sb_2O_{12}$. For system ZY3, a melted microstructure can be observed. These remarkable microstructural variations, found between 1000°C and 1100°C in the ZY2 and ZY3 systems, suggest the occurrence of a liquid-phase sintering process. On the other hand, for the ZY4 system, the microstructure at 1100°C remains the same as that at 1000°C.

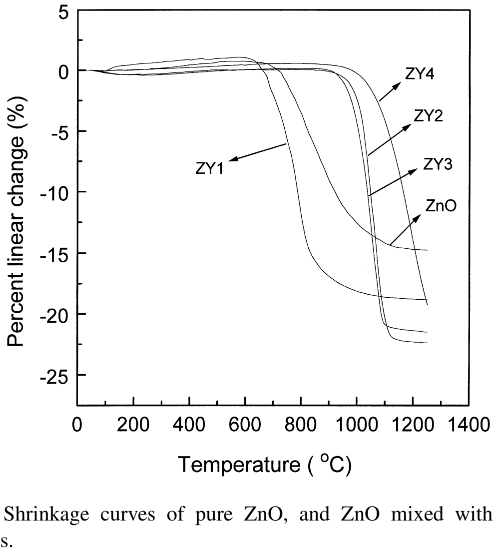

Fig. 3. Shrinkage curves of pure ZnO, and ZnO mixed with various additives.

3.3. Reactions occurring in the secondary phases-added ZnO

In order to investigate the correlation between the formed compounds and sintering behavior, the specimens were quenched at elevated temperatures. The XRD patterns of ZY3 system, quenched at 900°C, 1000°C, 1100°C, and 1250°C, are presented in Fig. 5. Notably, the ZY3 system consists of ZnO and pyrochlore phase $ZnBi_{1.5}Sb_{1.5}O_7$. At 900°C, only $ZnBi_{1.5}Sb_{1.5}O_7$ coexists with ZnO; while at 1000°C, a small amount of α-$Zn_7Sb_2O_{12}$ is formed. From 1100°C, the amount of $ZnBi_{1.5}Sb_{1.5}O_7$ rapidly decreases and β-$Zn_7Sb_2O_{12}$ is formed. On heating further to 1250°C, nearly all $ZnBi_{1.5}Sb_{1.5}O_7$ is consumed, and β-$Zn_7Sb_2O_{12}$ and Bi_2O_3 are formed. The results in Figs. 3 and 5 reveal that the rapid shrinkage and remarkable microstructural variations in ZY3 is caused by the reaction between the pyrochlore phase and ZnO.

Variations in the relative amounts of secondary compounds formed in systems ZY2, ZY3, and ZY4 are shown in Fig. 6. It is found that, at 1000°C $ZnBi_{1.5}Sb_{1.5}O_7$ is present in ZY2 system. However, after 1100°C heating, β-$Zn_7Sb_2O_{12}$ is formed, along with a decrease in $ZnBi_{1.5}Sb_{1.5}O_7$. Therefore, in ZY2 and ZY3 systems, the following reaction, proposed by Inada [11], is believed to occur:

$$17ZnO + 4ZnBi_{1.5}Sb_{1.5}O_7 \rightarrow 3\beta\text{-}Zn_7Sb_2O_{12} + 3Bi_2O_3 \quad (1)$$

The presence of pyrochlore phase in ZY2 and ZY3 plays a similar role in the sintering of ZnO, regardless of whether pyrochlore phase is added to ZnO (in ZY3) or produced by the reactions between the additives and ZnO (in ZY2). When pyrochlore phase reacts with ZnO at 1000°C, β-$Zn_7Sb_2O_{12}$ and Bi_2O_3 are formed. The latter compound accelerates the sintering rate of ZnO through a liquid-phase sintering mechanism. The melting point of pyrochlore phase

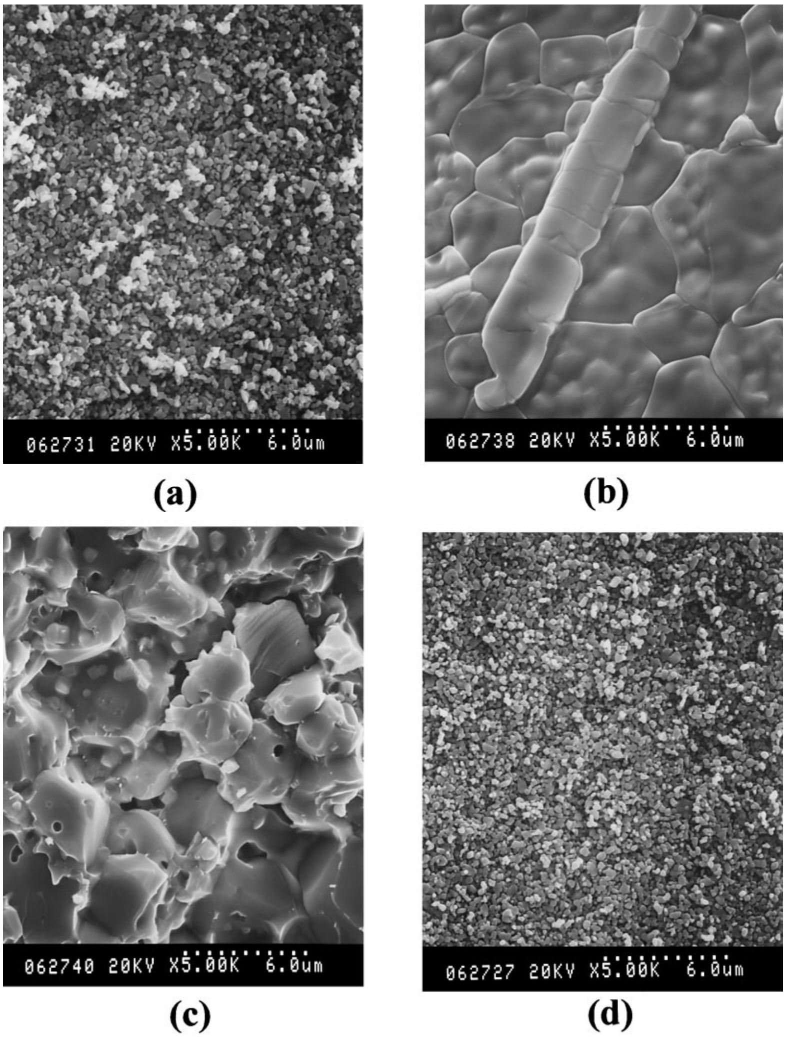

Fig. 4. Scanning electron micrographs of (a) ZY2 quenched at 1000°C, and (b) ZY2, (c) ZY3 and (d) ZY4 quenched at 1100°C.

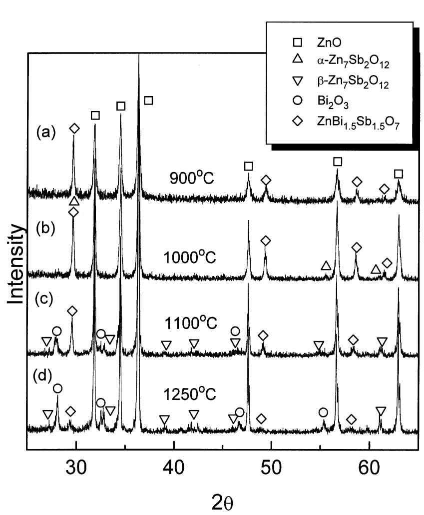

Fig. 5. X-ray diffraction patterns of ZY3 quenched at (a) 900°C, (b) 1000°C, (c) 1100°C, and (d) 1250°C.

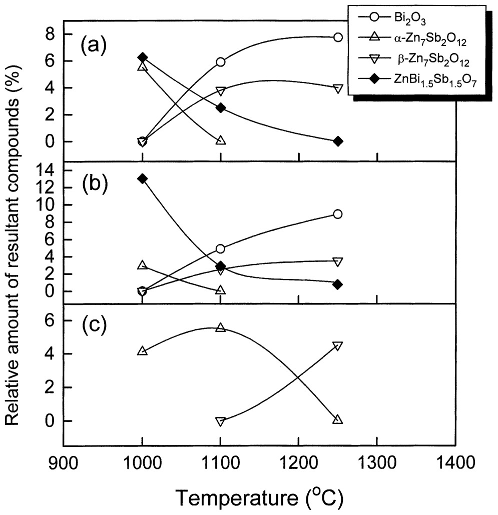

Fig. 6. Variations in the relative amounts of secondary compounds formed in (a) ZY2, (b) ZY3, and (c) ZY4 as a function of temperature.

has been reported to be 1280°C [11]. Therefore, the rapid shrinkage of ZY2 and ZY3 systems at around 1000°C (Fig. 3) is caused by the reaction between ZnO and pyrochlore phase, rather than the direct melting of the pyrochlore phase. The remarkable microstructural variations (Fig. 4) in the ZY2 and ZY3 systems are confirmed to result from the formation of liquid phase through the reaction of pyrochlore phase.

In the ZY4 system, no pyrochlore phase is formed at elevated temperatures, and, consequently, no rapid shrinkage is observed around 1000°C. Only α and β-$Zn_7Sb_2O_{12}$ compounds are found to coexist in the ZY4 system. β-$Zn_7Sb_2O_{12}$ is formed from the phase transformation of α-$Zn_7Sb_2O_{12}$, rather than from the reaction between ZnO and pyrochlore phase. Apparently, the spinel phase α-$Zn_7Sb_2O_{12}$ does not react with ZnO to form secondary phases. Furthermore, based on the results in Figs. 3 and 4, the presence of spinel phase appears to postpone the sintering process, and hinders the growth of ZnO grains.

4. Conclusions

The shrinkage behavior of ZnO-based varistors has been investigated in this study. With the addition of Bi_2O_3 and Sb_2O_3, the specimen rapidly shrinks from 1000°C. The rapid shrinkage is related to the reaction between the pyrochlore phase and ZnO. This reaction has been confirmed by investigating the system of ZnO and a synthesized pyrochlore phase ($ZnBi_{1.5}Sb_{1.5}O_7$ with $a_o = 10.4438$ Å). This pyrochlore phase is found to react with ZnO at 1000°C to result in the formation of Bi_2O_3, which accelerates the sintering rate of ZnO through a liquid-phase sintering mechanism. On the other hand, addition of spinel phase α-$Zn_7Sb_2O_{12}$ not only postpones the sintering process of ZnO, but also hinders the growth of ZnO grains.

References

[1] M. Matsuoka, Jpn. J. Appl. Phys. 10 (1971) 736.
[2] L.M. Levinson, H.R. Philip, IEEE Trans. Parts. Hybrid Packaging PAP-13 (1977) 338.
[3] K. Eda, J. Appl. Phys. 51 (1980) 4453.
[4] A. Kusy, T.G.M. Kleinpenning, J. Appl. Phys. 54 (1983) 2900.
[5] A. Miralles, A. Cornet, A. Herma, J.R. Morante, Mater. Sci. Eng. A 109 (1989) 201.
[6] Y.C. Chen, C.Y. Shen, H.Z. Chen, Y. Fang, L. Wu, Jpn. J. Appl. Phys. 30 (1991) 84.
[7] S.A. Pianaro, E.C. Pereira, L.O.S. Bulhoes, E. Longo, J.A. Varela, J. Mater. Sci. 30 (1995) 133.
[8] K. Eda, IEEE Electr. Insulation 5 (1989) 28.
[9] J. Wong, J. Appl. Phys. 46 (1975) 1653.
[10] M. Inada, Jpn. J. Appl. Phys. 17 (1978) 1.
[11] M. Inada, Jpn. J. Appl. Phys. 19 (1980) 409.
[12] J.C. Kim, E. Goo, J. Mater. Sci. 24 (1989) 76.
[13] T. Asokan, R. Freer, J. Mater. Sci. 25 (1990) 2447.